

# PFGE: Parsimonious Fast Geometric Ensembling of DNNs

Hao Guo, Jiyong Jin, and <sup>\*</sup>Bin Liu

Research Center for Applied Mathematics and Machine Intelligence,  
Zhejiang Lab, Hangzhou, 311121 China  
`{guoh, jinjy, liubin}@zhejianglab.com`

**Abstract** Ensemble methods have been widely used to improve the performance of machine learning methods in terms of generalization, while they are hard to use in deep learning systems, as training an ensemble of deep neural networks (DNNs) incurs an extremely higher computational overhead of model training. Recently, advanced techniques such as fast geometric ensembling (FGE) and snapshot ensemble have been proposed. These methods can train the model ensembles in the same time as a single model, thus getting around the hurdle of training time. However, their memory overhead for test-time inference remains much higher than single model based methods. Here we propose a parsimonious FGE (PFGE) that employs a lightweight ensemble of higher-performing DNNs, generated by successively-performed stochastic weight averaging procedures. Experimental results across different modern DNN architectures on widely used image datasets CIFAR- $\{10, 100\}$  and Imagenet, demonstrate that PFGE is 5x memory efficient than prior art methods, yet without compromise in generalization. Our code is available at <https://github.com/ZJLAB-AMMI/PFGE>.

**Keywords:** deep learning · ensemble method · generalization

## 1 Introduction

Ensemble methods have been widely used to improve the generalization performance of machine learning methods [4,27,2,5]. However, they are hard to apply in learning with modern deep neural networks (DNNs). A modern DNN often has millions, even billions, of parameters. A direct ensembling of  $k$  DNNs leads to a  $k$ -folded computational overhead in terms of training time and memory requirement for test-time inference. Recently, the fast geometric ensembling (FGE) and snapshot ensemble (SNE) methods are proposed, which can train an ensemble of DNNs in the same time as a single model, thus getting around the hurdle of training time [8,14]. However, their memory overhead for test-time inference remains much higher than single model based methods. To reduce the test-time cost of ensembles, authors of [1,13] propose methods for model compression and knowledge distillation, which aim to train one single model to encompass the

---

<sup>\*</sup> Correspondence author

“knowledge” of the ensembles. However, such methods do not consider the computational overhead of ensemble training.

In this paper, we consider: *how to reduce the training time cost and the test-time memory budget together, for DNN model ensembling?* This issue is crucially important especially for resource-constrained application scenarios of DNNs. In particular, we propose a novel algorithm referred to as PFGE, which is 5x memory efficient than prior art methods for test-time inference, yet without compromise in generalization and training efficiency. In another word, PFGE achieves the goal of simultaneously reducing the training-time and the test-time computational budgets for DNN ensembling without compromising generalization performance.

The remainder of this paper is organized as follows. In Section 2, we present related works. In Section 3, we introduce the proposed PFGE algorithm. In Section 4, we present the experimental results. Finally, we conclude the paper in Section 5.

## 2 Related Works

Ensemble methods are often computationally intractable for learning with modern DNNs, due to an extremely high overhead of ensemble training and test-time inference. Nevertheless, notable advances have been made to adapt ensemble methods to DNNs, such as FGE [8], SNE [14], SWA-Gaussian (SWAG) [21], Monte-Carlo dropout [7], and deep ensembles [6,19]. Among them, FGE, SNE and SWAG are most related to this work, as they all employ a cyclical learning rate (LR), and train DNN ensembles in the same time as for one DNN model.

Both FGE and SNE build DNN ensembles by sampling network weights from an SGD trajectory corresponding to a cyclical LR [24]. Running an SGD with a cyclical LR is in principle equivalent to SGD sampling with periodic warm restarts [20]. Authors of [14,8] demonstrate that the cyclical LR indeed provides a highly efficient way to collect high-quality DNN weights, which define the models for ensembling.

Compared with SNE, FGE is featured by a geometric explanation of its way to generating the ensembles. Specifically, FGE is inspired by one geometric insight about the DNN loss landscape, which says that there exist simple curves that connect local optima, and over these curves, both the training accuracy and the test accuracy remain approximately constant. FGE provides an efficient way to discover the high-accuracy pathways between local optima.

Inspired by FGE, SWA is proposed, which averages the high-performing network weights yielded by FGE for test-time inference [16]. The geometric insight underlying SWA is that averaging weights sampled from an SGD trajectory corresponding to a cyclical or constant LR can find wider optima, and wider optima lead to better generalization [17]. SWAG uses the SWA solution as the center of a Gaussian distribution, which is formed to approximate the posterior of the network weights [21]. SWAG generates the model ensembles by sampling from this Gaussian.

### 3 The Proposed PFGE Algorithm

The design of PFGE is inspired by an observation that running one stochastic weight averaging (SWA) procedure can lead to a higher-performing local optimum [16], and running a series of SWA procedures successively may find a set of higher-performing weights than those obtained with SGD [10]. FGE employs an ensemble of models found by SGD. We conjecture that, using an ensemble of higher-performing models found by SWA, PFGE could use much fewer models to yield a generalization performance on par with FGE. Experimental results, see Section 4, demonstrate that our conjecture indeed holds.

We present the pseudo-codes to implement SWA, FGE, and PFGE in Algorithms 1, 2, and 3, respectively. They all perform stochastic gradient based weight updating iteratively, starting at a local optimum  $w_0$  provided by an SGD that runs preceding them. The iterative weight updating operation employs a cyclical LR for letting the weight trajectory escape from the current optimum, and then discover and converge to novel local optima. A conceptual diagram of the cyclical LR is shown in Figure 1, where  $\alpha_1$  and  $\alpha_2$  bound the LR values,  $c$  denotes the cycle length,  $n$  the total number of allowable iterations that depends on the budget of training time,  $P$  the period to collect the member models for PFGE.

---

**Algorithm 1** SWA based model training and test-time prediction

---

**Input:** initial network weights  $w_0$ , cyclical LR schedule  $SC$ , cycle length  $c$ , budget (the total number of allowable iterations)  $n$ , test data  $x$

**Output:** predicted label  $y$  of  $x$

```

1:  $w \leftarrow w_0$ ; solution set  $\mathcal{S} \leftarrow \{\}$ .
2:  $w_{\text{SWA}} \leftarrow w$ .
3: for  $i \leftarrow 1, 2, \dots, n$  do
4:   Compute current learning rate  $\alpha$  according to  $SC$ .
5:    $w \leftarrow w - \alpha \nabla \mathcal{L}_i(w)$  (stochastic gradient update).
6:   if  $\text{mod}(i, c) = 0$  then
7:      $n_{\text{models}} \leftarrow i/c$  (number of models averaged).
8:      $w_{\text{SWA}} \leftarrow (w_{\text{SWA}} \cdot n_{\text{models}} + w) / (n_{\text{models}} + 1)$ .
9:   end if
10: end for
11: Input  $x$  into the DNN with weights  $w_{\text{SWA}}$ , then compute the its softmax output.
12: return  $y$  that maximizes the above softmax output.

```

---

The iterative weight updating operation employs a cyclical LR for letting the weight trajectory escape from the current optimum, and then discover and converge to novel local optima. A conceptual diagram of the cyclical LR is shown in Figure 1, where  $\alpha_1$  and  $\alpha_2$  bound the LR values,  $c$  denotes the cycle length,  $n$  the total number of allowable iterations that define the budget of training time,  $P$  the model recording period for PFGE.

---

**Algorithm 2** FGE based model training and test-time prediction

---

**Input:** initial network weights  $w_0$ , cyclical LR schedule  $SC$ , cycle length  $c$ , budget (the total number of allowable iterations)  $n$ , test data  $x$

**Output:** predicted label  $y$  of  $x$

- 1:  $w \leftarrow w_0$ ; solution set  $\mathcal{S} \leftarrow \{\}$ .
- 2: **for**  $i \leftarrow 1, 2, \dots, n$  **do**
- 3:   Compute current learning rate  $\alpha$  according to  $SC$ .
- 4:    $w \leftarrow w - \alpha \nabla \mathcal{L}_i(w)$  (stochastic gradient update).
- 5:   **if**  $\text{mod}(i, c) = 0$  **then**
- 6:     Add  $w$  into  $\mathcal{S}$  (collect weights).
- 7:   **end if**
- 8: **end for**
- 9: Given  $x$  as the input, compute the average of softmax outputs of models included in  $\mathcal{S}$ .
- 10: **return**  $y$  that maximizes the above averaged softmax output.

---



---

**Algorithm 3** PFGE based model training and test-time prediction

---

**Input:** initial network weights  $w_0$ , cyclical LR schedule  $SC$ , cycle length  $c$ , budget (the total number of allowable iterations)  $n$ , test data  $x$ , model recording period  $P$

**Output:** predicted label  $y$  of  $x$

- 1:  $w \leftarrow w_0$ ; solution set  $\mathcal{S} \leftarrow \{\}$ .
- 2:  $w_{\text{SWA}} \leftarrow w$ .
- 3:  $n_{\text{recorded}} \leftarrow 0$  (number of models recorded in  $\mathcal{S}$ ).
- 4: **for**  $i \leftarrow 1, 2, \dots, n$  **do**
- 5:   Compute current learning rate  $\alpha$  according to  $SC$ .
- 6:    $w \leftarrow w - \alpha \nabla \mathcal{L}_i(w)$  (stochastic gradient update).
- 7:    $j \leftarrow i - n_{\text{recorded}} \times P$  (iterate index for the follow-up SWA procedure).
- 8:   **if**  $\text{mod}(j, c) = 0$  **then**
- 9:      $n_{\text{models}} \leftarrow j/c$  (number of models that have been averaged within the current SWA procedure).
- 10:     $w_{\text{SWA}} \leftarrow (w_{\text{SWA}} \cdot n_{\text{models}} + w) / (n_{\text{models}} + 1)$ .
- 11:   **end if**
- 12:   **if**  $\text{mod}(i, P) = 0$  **then**
- 13:     Add  $w_{\text{SWA}}$  into  $\mathcal{S}$  (collect weights).
- 14:      $w \leftarrow w_{\text{SWA}}$  (initialization for the follow-up SWA procedure).
- 15:      $n_{\text{recorded}} \leftarrow i/P$  (number of models recorded in  $\mathcal{S}$ ).
- 16:   **end if**
- 17: **end for**
- 18: Given  $x$  as the input, compute the average of softmax outputs of models recorded in  $\mathcal{S}$ .
- 19: **return**  $y$  that maximizes the above averaged softmax output.

---

As shown in Algorithm 1, SWA maintains a running average of the network weights that are collected at every  $c$  iterations, and finally outputs a single model with weight  $w_{\text{SWA}}$  used for test-time inference.  $w_{\text{SWA}}$  is in fact the average of  $(\frac{n}{c})$  weights traversed along the SGD trajectory.

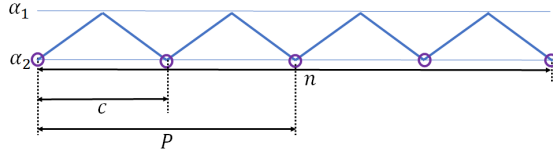


**Figure 1.** A conceptual diagram of the cyclical LR used by SWA, FGE and PFGE. The circles mask the time instances for recording the local optima discovered along the SGD trajectory. The real relationship between  $c$ ,  $P$ , and  $n$  is that  $P$  is an integer multiple of  $c$ , and  $n$  is an integer multiple of  $P$ . Here only one example case is plotted, in which  $P = 2c$  and  $n = 2P$ . See the text for detailed explanations for all parameters involved.

PFGE differentiates with FGE in the way to generate the ensemble models. For FGE, its ensemble models are generated purely by SGD (see operations 4 and 6 in Algorithm 2), while PFGE resorts to multiple SWA operations performed in succession (see operations 10 and 13 in Algorithm 3) to generate the models. In the successively performed SWA procedures, the output of an SWA procedure is used to initialize its follow-up SWA procedure (see operation 14 in Algorithm 3). The code to implement PFGE is available at <https://github.com/ZJLAB-AMMI/PFGE>.

## 4 Experiments

We compare PFGE against SOTA methods FGE [8], SWA [16], and SWAG [21], on CIFAR-10 [18], CIFAR-100 [18], and ImageNet ILSVRC-2012 [3,22], to test its generalization performance in terms of test accuracy. We also test its capability for uncertainty calibration, and conduct mode connectivity test for PFGE, while the experimental results are deferred to the Appendix Section.

### 4.1 Experimental Setting

As shown in Algorithms 1-3, SWA, FGE, and PFGE are all initialized with a local optimum  $w_0$  and an LR schedule. For all architectures and datasets, we initialize all algorithms in comparison with the same  $w_0$ , and the same LR setting. Following [8], we use a triangle LR schedule, as shown in Figure 1. Specifically, we set  $c$  to iteration numbers corresponding to 2 or 4 epochs (following [8]),  $P$  to 10 epochs, and  $n$  to 40 or 20 epochs. For  $\alpha_1$ , and  $\alpha_2$ , we set them in the same way as in [8]. The mini-batch size for model training is fixed at 128.

For CIFAR-{10, 100}, we obtain  $w_0$  from running a standard SGD with momentum affiliated by the same type of decaying LR schedule as used in [16], to minimize an  $L2$ -regularization based cross-entropy loss, until convergence. We

set the hyperparameters of SGD, e.g., the weight decaying parameter, the momentum factor, in the same way as in [16]. For ImageNet, we use pre-trained models ResNet-50 [11], ResNet-152 [11], and DenseNet-161 [15] contained in PyTorch to initialize  $w_0$  and fixes  $n$  to be the iteration number that corresponds to 40 epochs.

In our experiments, PFGE always employs 4 model components. It uses the average of those 4 models' softmax outputs for test-time prediction. For FGE and SWAG, we compute test-time predictions by averaging softmax outputs of last 4 models that have been added into their ensemble set  $\mathcal{S}$ . By this, we guarantee that all algorithms have roughly the same overhead of test-time inference. For reference, we also present results of FGE-whole and SWAG-whole, corresponding to FGE and SWAG that use the whole ensemble, i.e., 20 models, for test-time inference. The considered performance metrics is test accuracy.

## 4.2 CIFAR Datasets

We experiment with network architectures VGG16 [23], Preactivation ResNet-164 (PreResNet-164) [12], WideResNet-28-10 [26] on CIFAR-10, 100.

We run each algorithm at least 3 times independently, and report the averaged results of test accuracy, and the corresponding standard error in Tables 1 and 2. On CIFAR-10, we find that for VGG16, PFGE has the highest test ac-

**Table 1.** Test accuracy on CIFAR-10. Best results for each architecture are **bolded**.

Algorithm	Test Accuracy (%)		
	VGG16	PreResNet	WideResNet
PFGE	<b>93.41</b> $\pm$ 0.08	95.70 $\pm$ 0.05	96.37 $\pm$ 0.03
FGE	93.03 $\pm$ 0.18	95.52 $\pm$ 0.08	96.14 $\pm$ 0.07
SWA	93.33 $\pm$ 0.02	<b>95.78</b> $\pm$ 0.07	<b>96.47</b> $\pm$ 0.04
SWAG	93.24 $\pm$ 0.06	95.45 $\pm$ 0.14	96.36 $\pm$ 0.04
FGE-whole	93.40 $\pm$ 0.08	95.57 $\pm$ 0.05	96.27 $\pm$ 0.02
SWAG-whole	93.37 $\pm$ 0.07	95.61 $\pm$ 0.11	96.45 $\pm$ 0.07

**Table 2.** Test accuracy on CIFAR-100. Best results for each architecture are **bolded**.

Algorithm	Test Accuracy (%)		
	VGG16	PreResNet	WideResNet
PFGE	<b>74.17</b> $\pm$ 0.04	<b>80.06</b> $\pm$ 0.13	<b>81.96</b> $\pm$ 0.01
FGE	73.49 $\pm$ 0.24	79.76 $\pm$ 0.06	81.09 $\pm$ 0.25
SWA	73.83 $\pm$ 0.20	79.97 $\pm$ 0.06	81.92 $\pm$ 0.02
SWAG	73.77 $\pm$ 0.18	79.24 $\pm$ 0.04	81.55 $\pm$ 0.06
FGE-whole	74.34 $\pm$ 0.05	80.17 $\pm$ 0.09	81.62 $\pm$ 0.16
SWAG-whole	74.15 $\pm$ 0.17	80.00 $\pm$ 0.03	81.83 $\pm$ 0.12

curacy (93.41%). For PreResNet-164 and WideResNet-28-10, PFGE beats FGE and SWAG but loses to SWA in terms of test accuracy; SWA achieves the highest accuracy (95.78% and 96.47%). On CIFAR-100, we find that PFGE performs best in terms of test accuracy for all network architectures. We also find from Tables 1 and 2 that, even compared with FGE-whole and SWAG-whole, PFGE achieves a comparable even better performance in terms of test accuracy, yet requires only 20% memory overhead for test-time inference.

### 4.3 IMAGENET

We experiment with network architectures ResNet-50 [11], ResNet-152 [11], and DenseNet-161 [15] on ImageNet ILSVRC-2012 [3,22]. The same as before, we run each algorithm 3 times independently.

The result is shown in Table 3. We see that PFGE outperforms FGE and SWAG, and performs comparatively to FGE-whole and SWAG-whole, in terms of test accuracy.

**Table 3.** Test accuracy on Imagenet. Best results for each architecture are **bolded**.

Algorithm	Test Accuracy (%)		
	ResNet-50	ResNet-152	DenseNet-161
PFGE	<b><math>77.06 \pm 0.19</math></b>	<b><math>79.07 \pm 0.04</math></b>	<b><math>78.72 \pm 0.08</math></b>
FGE	$76.85 \pm 0.07$	$78.73 \pm 0.02$	$78.53 \pm 0.08$
SWA	$76.70 \pm 0.38$	$78.82 \pm 0.02$	$78.41 \pm 0.29$
SWAG	$76.19 \pm 0.29$	$78.72 \pm 0.04$	$77.19 \pm 0.83$
FGE-whole	$77.17 \pm 0.08$	$79.13 \pm 0.06$	$78.91 \pm 0.06$
SWAG-whole	$76.70 \pm 0.35$	$79.10 \pm 0.06$	$77.94 \pm 0.62$

### 4.4 Performance of separate models in the ensemble

We check the performance of each separate model in PFGE and FGE. Each separate model can be seen as a “snapshot” of the SGD trajectory. We collect such “snapshot” models at a set of training checkpoints, and then compute their generalization performances in terms of test accuracy. The result is shown in Fig.2, wherein the term FGE corresponds to FGE-whole in Tables 2 and 3. From Fig. 2, we find that:

- the separate models of PFGE are indeed higher-performing than those of FGE, in terms of test accuracy, for both datasets and for all network architectures considered;
- for PFGE and FGE, the more member models are used, the higher is the test accuracy given by the model ensemble.

The experimental results indicate that, thanks to the higher-quality of the separate model components, PFGE performs better than FGE and SWAG if they

are equipped with the same number of model components, and even equipped with much fewer model components, PFGE performs on par with FGE-whole and SWAG-whole.

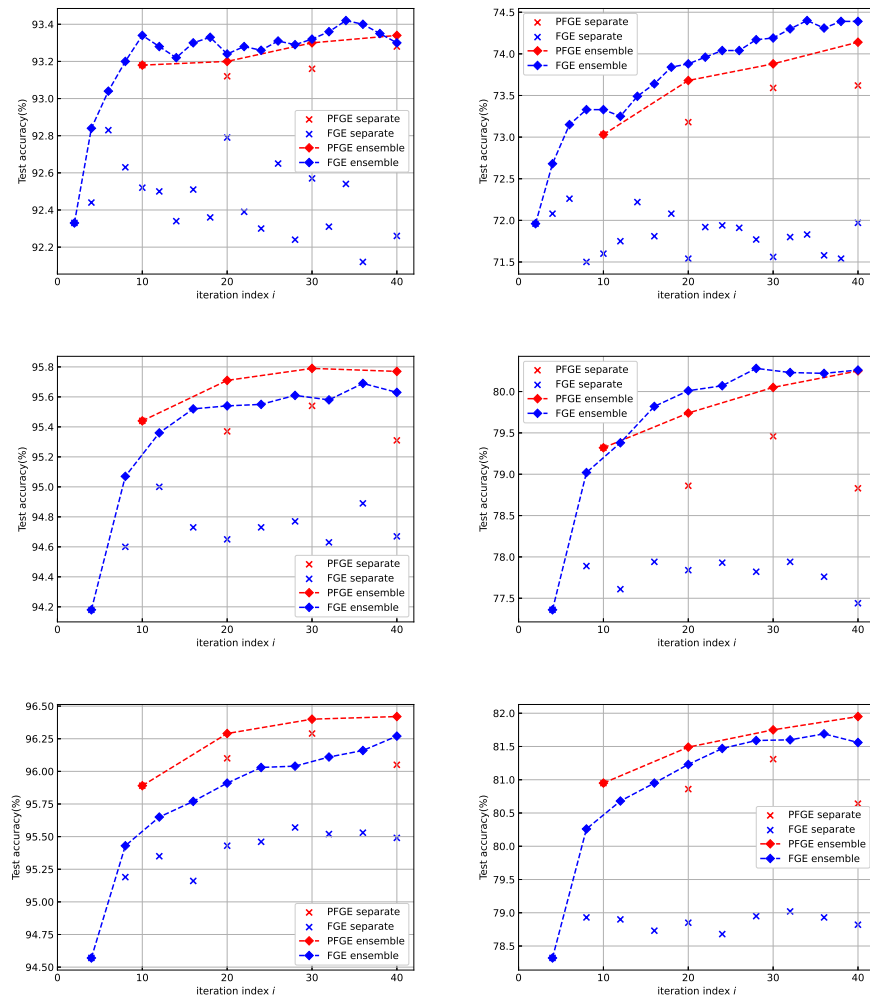


**Figure 2.** Ensemble performance of PFGE and FGE as a function of the training iteration index  $i$ . Crosses represent the performance of separate “snapshot” models, and diamonds show the performance of the ensembles composed of all models available at the given iteration. Left column: CIFAR-10. Right column: CIFAR-100. Top row: VGG16. Middle Row: PreResNet-164. Bottom row: WideResNet-28-10.

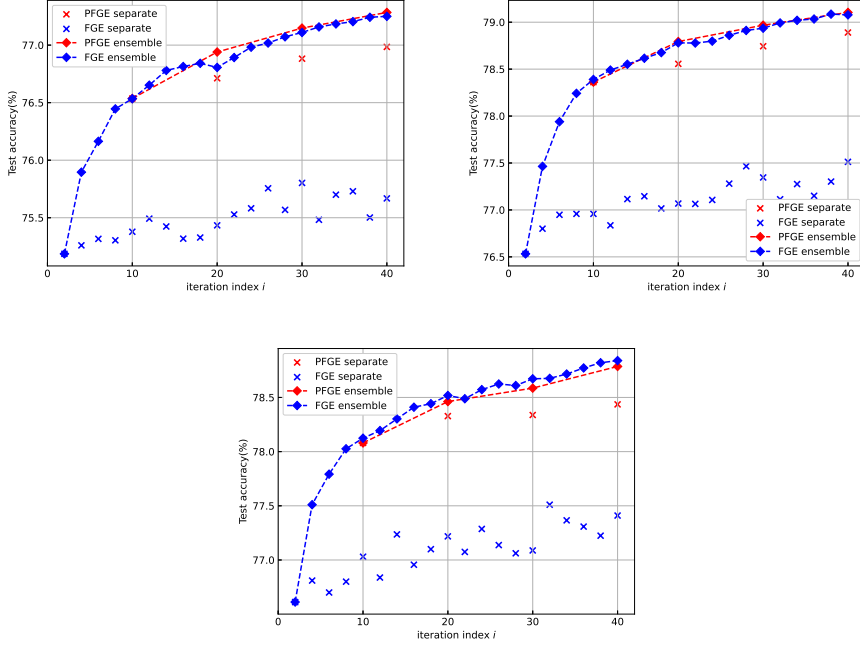


**Figure 3.** Ensemble performance of PFGE and FGE on Imagenet as a function of the training iteration index  $i$ . Top Left: ResNet-50. Top Right: ResNet-152. Bottom: DenseNet-161. Crosses represent the performance of separate “snapshot” models, and diamonds show the performance of the ensembles composed of all models available at the given iteration.

#### 4.5 On Uncertainty Calibration

We conduct experiments to test PFGE’s capability for uncertainty calibration both numerically and visually through the reliability diagram. We find that PFGE’s capability for uncertainty calibration is better than SWA, while worse than FGE-whole. Specifically we compare PFGE against FGE, SWA, and SWAG, on CIFAR-10, CIFAR-100, and ImageNet ILSVRC-2012, to test its capability for uncertainty calibration. The considered performance metrics include negative log-likelihood (NLL), and the expected calibration error (ECE) [9]. These metrics are used for evaluating an algorithm’s capability for uncertainty calibration in [9,21]. We run each algorithm at least 3 times independently, and report the averaged results of NLL, and ECE, and the corresponding standard error in Tables 4, 5, and 6. We also plot reliability diagrams in Figure 4, in which FGE and SWAG respectively correspond to FGE-whole and SWAG-whole in Tables 4 and 5. The results demonstrate FGE-whole’s advantage and SWA’s shortage for uncertainty calibration, and show that PFGE behaves in between them in terms of calibration.

**Table 4.** NLL and ECE on CIFAR-10. The best results for each architecture are **bolded**.

Algorithm	NLL			ECE		
	VGG16	PreResNet	WideResNet	VGG16	PreResNet	WideResNet
PFGE	26.16 $\pm$ 0.08	<b>13.05</b> $\pm$ 0.10	<b>11.04</b> $\pm$ 0.05	3.80 $\pm$ 0.08	0.54 $\pm$ 0.15	0.62 $\pm$ 0.02
FGE	25.25 $\pm$ 0.60	13.60 $\pm$ 0.11	11.73 $\pm$ 0.15	3.12 $\pm$ 0.09	0.49 $\pm$ 0.09	0.32 $\pm$ 0.08
SWA	28.06 $\pm$ 0.20	13.50 $\pm$ 0.07	11.22 $\pm$ 0.11	4.44 $\pm$ 0.07	1.21 $\pm$ 0.09	11.33 $\pm$ 0.04
SWAG	24.58 $\pm$ 0.06	13.71 $\pm$ 0.13	11.43 $\pm$ 0.19	3.21 $\pm$ 0.03	0.75 $\pm$ 0.12	1.03 $\pm$ 0.05
FGE-whole	<b>21.89</b> $\pm$ 0.53	13.07 $\pm$ 0.10	11.18 $\pm$ 0.06	<b>2.24</b> $\pm$ 0.08	<b>0.39</b> $\pm$ 0.06	<b>0.30</b> $\pm$ 0.08
SWAG-whole	23.10 $\pm$ 0.29	13.12 $\pm$ 0.08	11.07 $\pm$ 0.17	3.01 $\pm$ 0.10	0.53 $\pm$ 0.09	0.78 $\pm$ 0.05

**Table 5.** NLL and ECE on CIFAR-100. The best results for each architecture are **bolded**.

Algorithm	NLL			ECE		
	VGG16	PreResNet	WideResNet	VGG16	PreResNet	WideResNet
PFGE	132.85 $\pm$ 0.19	72.07 $\pm$ 0.34	65.00 $\pm$ 0.14	13.95 $\pm$ 0.07	5.05 $\pm$ 0.23	4.24 $\pm$ 0.02
FGE	125.77 $\pm$ 0.20	72.75 $\pm$ 0.18	68.91 $\pm$ 0.18	11.80 $\pm$ 0.19	3.41 $\pm$ 0.12	2.84 $\pm$ 0.32
SWA	143.23 $\pm$ 0.57	76.88 $\pm$ 0.43	69.57 $\pm$ 0.39	16.42 $\pm$ 0.29	7.56 $\pm$ 0.14	6.89 $\pm$ 0.12
SWAG	122.87 $\pm$ 0.88	74.37 $\pm$ 0.14	68.09 $\pm$ 0.25	11.20 $\pm$ 0.03	4.74 $\pm$ 0.03	5.22 $\pm$ 0.07
FGE-whole	<b>109.93</b> $\pm$ 0.51	<b>69.26</b> $\pm$ 0.23	<b>63.54</b> $\pm$ 0.24	<b>8.84</b> $\pm$ 0.01	<b>1.92</b> $\pm$ 0.19	<b>1.15</b> $\pm$ 0.04
SWAG-whole	117.25 $\pm$ 0.62	71.07 $\pm$ 0.15	66.37 $\pm$ 0.29	10.99 $\pm$ 0.11	3.36 $\pm$ 0.05	4.65 $\pm$ 0.11

**Table 6.** NLL and ECE on Imagenet. The best results for each architecture are **bolded**.

Algorithm	NLL			ECE		
	ResNet-50	ResNet-152	DenseNet-161	ResNet-50	ResNet-152	DenseNet-161
PFGE	<b>81.08</b>	81.08	<b>82.03</b>	2.00	2.61	1.84
FGE	90.47	81.91	82.87	1.59	<b>1.54</b>	<b>1.51</b>
SWA	90.90	83.40	83.47	3.43	4.10	2.46
SWAG	92.02	82.00	84.91	<b>1.54</b>	1.85	3.22
FGE-whole	88.62	80.21	81.31	2.19	2.43	2.54
SWAG-whole	88.94	<b>80.19</b>	82.85	1.73	1.65	3.35

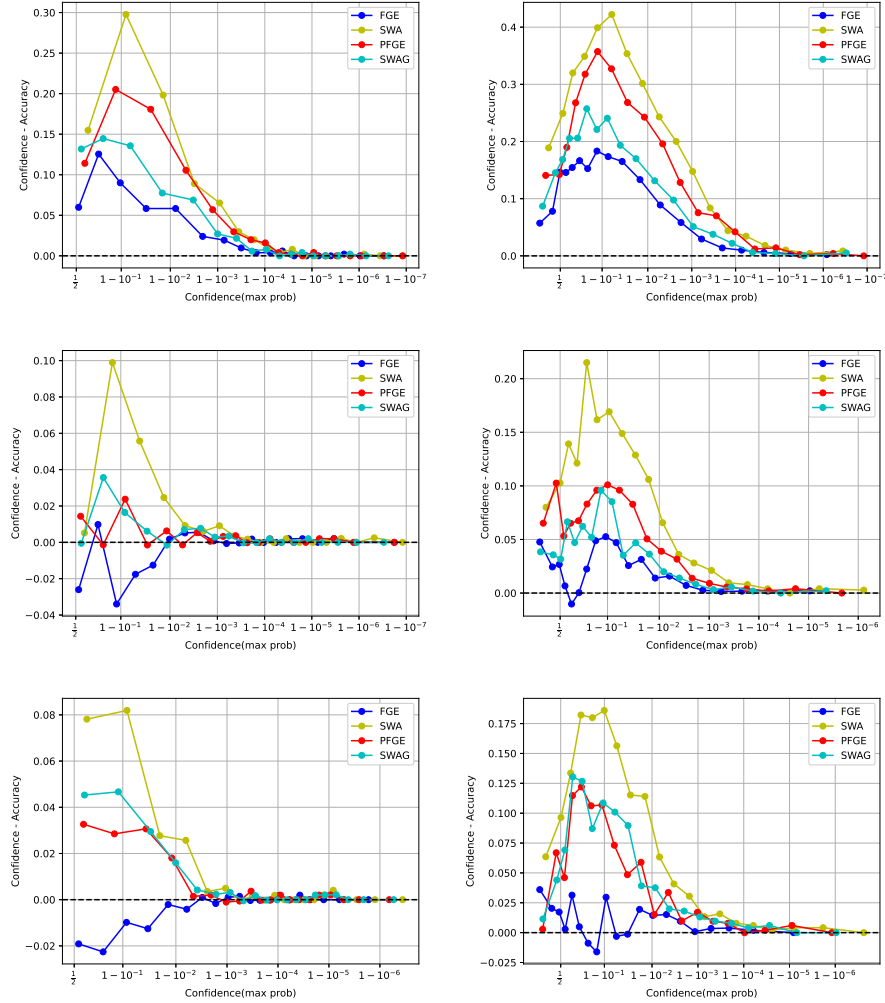


**Figure 4.** Reliability diagrams. Left column: CIFAR-10. Right column: CIFAR-100. Top row: VGG16. Middle Row: PreResNet-164. Bottom row: WideResNet-28-10

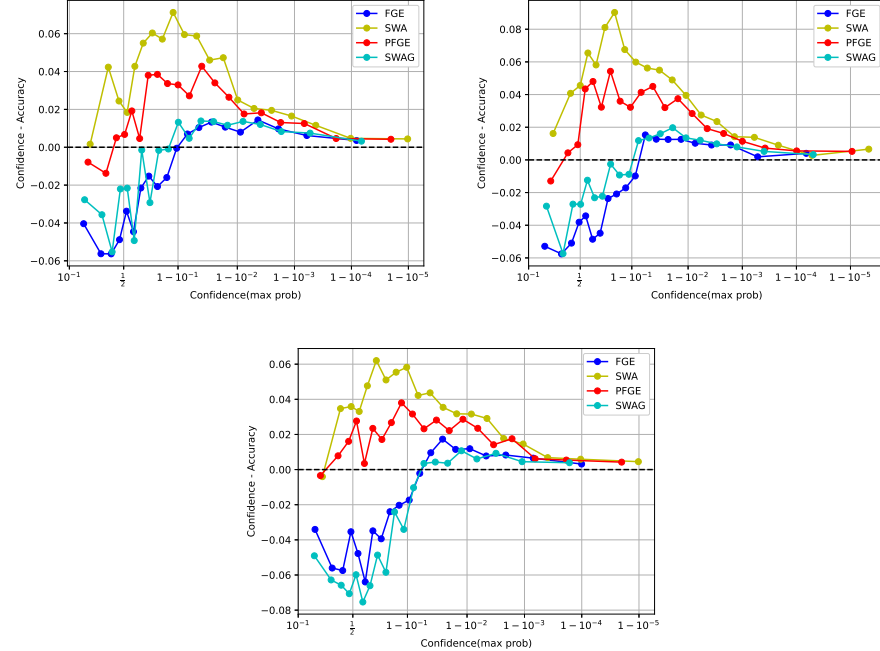


**Figure 5.** Reliability diagrams on Imagenet. Top Left: ResNet-50. Top Right: ResNet-152. Bottom Row: DenseNet-161.

#### 4.6 Mode Connectivity Test

In [25], the authors demonstrate that, when ensembles of trained models converge to locally smooth regions of the loss landscape, the best test accuracy is obtained. That means, the mode connectivity of its model components closely relates to the ensemble’s generalization performance. We conduct an experiment to test the mode connectivity of PFGE’s model components against that of FGE’s. We find that the mode connectivity of model components given by PFGE is better than FGE.

Specifically, we randomly select a pair of neighboring model components, denoted by  $w$  and  $w'$ , in the ensemble set  $\mathcal{S}$ . Given  $w$  and  $w'$ , we first search a low-energy curve  $\gamma(t)$ ,  $t \in [0, 1]$ , for which  $\gamma(0) = w$ ,  $\gamma(1) = w'$ , which minimizes  $\int_0^1 \mathcal{L}(\gamma(t))dt$ , where  $\mathcal{L}$  denotes the DNN loss function. Following [25,8], we approximate  $\int_0^1 \mathcal{L}(\gamma(t))dt$  with  $\mathbb{E}_{t \sim U(0,1)} \mathcal{L}(\gamma_\phi(t))$ , and use the Bezier curve with  $k+1$  bends, given by  $\gamma_\phi(t) = \sum_{j=0}^k \binom{k}{j} (1-t)^{k-j} t^j w_j$  for  $t \in [0, 1]$ , where  $U(0, 1)$  denotes a continuous uniform distribution between 0 and 1,  $w_0 = w, w_k = w'$ , and  $\phi = \{w_1, \dots, w_{k-1}\}$  are parameters of additional models to be trained. Given the curve  $\gamma_\phi(t)$ , the mode connectivity of the models  $w, w'$  is defined to

be [25]

$$mc(w, w') = \frac{1}{2}(\mathcal{L}(w) + \mathcal{L}(w')) - \mathcal{L}(\gamma_\phi(t^*)), \quad (1)$$

where  $t^*$  maximizes the function  $f(t) \triangleq |\frac{1}{2}(\mathcal{L}(w) + \mathcal{L}(w')) - \mathcal{L}(\gamma_\phi(t))|$ .

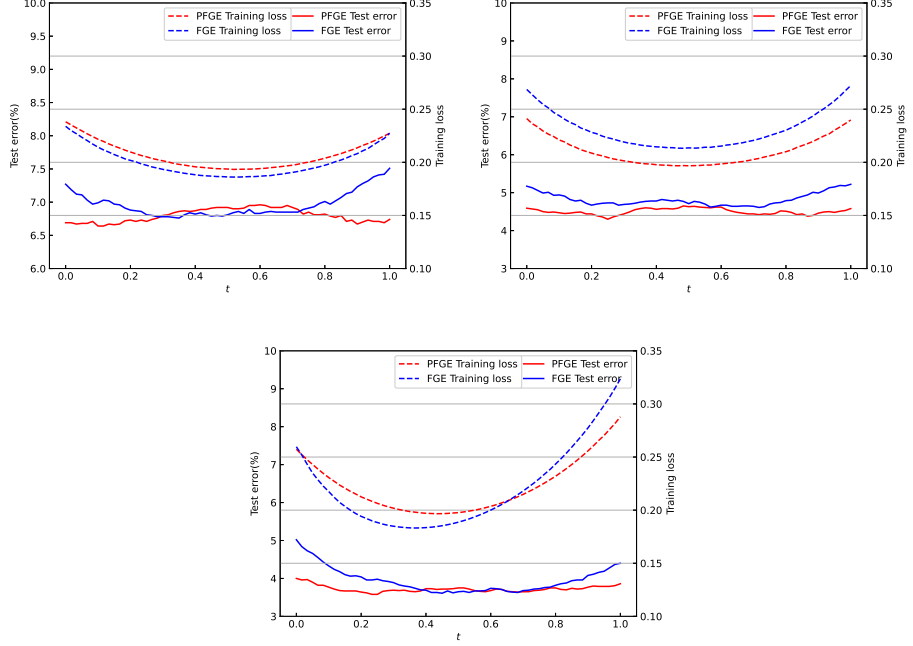


**Figure 6.** Test error and training loss on CIFAR-10 corresponding to  $\gamma_\phi(t)$  as a function of  $t$ . Top left: VGG16. Top right: PreResNet-164. Bottom: WideResNet-28-10.

**Table 7.** Statistics for test errors (%) of  $\gamma_\phi(t)$  on CIFAR-10. The test error values are collected along the changes of the  $t$  value from 0 to 1.

Architecture	Max		Min		Mean	
	PFGE	FGE	PFGE	FGE	PFGE	FGE
VGG16	6.96	7.51	6.64	6.76	6.76	6.99
PreResNet	4.65	5.22	4.30	4.61	4.50	4.82
WideResNet	4.14	4.53	3.43	3.63	3.63	3.87

We use the same computational procedure and hyperparameter setting in [25,8] to minimize the loss on the curve. We record the training loss and test

error values as a function of  $t$ , and plot them in Figure 6. The related statistics is shown in Tables 7 and 8. In Figure 6, we find that the training loss curve of PFGE has a consistent lower energy than that of FGE for VGG16 and PreResNet-164. The test error curve of PFGE is below that of FGE for most  $t$  values, for all architectures. The results in Tables 7 and 8 also show a consistent advantage of PFGE over FGE in terms of both test error and training loss.

The corresponding mc values are presented in Table 9, which shows that the model connectivity of PFGE is greater than that of FGE, for all architectures.

**Table 8.** Statistics for training losses of  $\gamma_\phi(t)$  on CIFAR-10. The training loss values are collected along the changes of the  $t$  value from 0 to 1.

Architecture	Max		Min		Mean	
	PFGE	FGE	PFGE	FGE	PFGE	FGE
VGG16	0.238	0.234	0.193	0.186	0.207	0.199
PreResNet	0.241	0.272	0.197	0.213	0.210	0.230
WideResNet	0.284	0.324	0.217	0.238	0.238	0.266

**Table 9.** Mode connectivity test on CIFAR-10. See the definition of mc in Equation (1). A mc value closer to 0 indicates a better mode connectivity and vice versa. See more details on the relationship between the value of mc and mode connectivity in [25]. The best results for each architecture are **bolded**.

Algorithm	mc value		
	VGG16	PreResNet	WideResNet
PFGE	<b>0.039</b>	<b>0.044</b>	<b>0.065</b>
FGE	0.045	0.057	0.084

#### 4.7 On training efficiency and test-time cost

As mentioned in Sec.4.1, all methods share the same LR setting, run the same number of SGD iterations, having the same training efficiency (in terms of training time). Their test-time cost (mainly in terms of memory overhead) is proportional to the number of member models in use, denoted by  $K$  here. For PFGE, we have  $K = (\frac{n}{P}) = 4$ . In contrast, for FGE [8] and SWAG [21] (namely FGE-whole and SWAG-whole in our experiments), we have  $K = (\frac{n}{c}) = 20$  according to our experimental setting in Sec.4.1. That means, using PFGE only requires only  $\frac{4}{20} = 20\%$  memory overhead for test-time inference compared with FGE [8] and SWAG [21]. In terms of test-time efficiency, SWA [16] is the optimal choice, since it always outputs a single model for use, namely  $K = 1$ . However, compared with ensemble methods, SWA suffers from uncertainty calibration, as shown in [21] and Section 4.5.

## 5 Conclusions

In this paper, we proposed a novel algorithm referred to as PFGE, which is a generic and architecture-agnostic approach to DNN model ensembling. Through experiments on the widely used image datasets CIFAR- $\{10, 100\}$  and Imagenet, we demonstrated that the memory efficiency of PFGE can achieve 5 times that of prior art methods FGE and SWAG without compromising the generalization performance. We tested the mode connectivity of model components given by PFGE, finding that it is better than that of FGE. This provides a geometric explanation for why PFGE beats FGE if they are equipped with the same number of model components. We also investigated the involved algorithms' performance in terms of uncertainty calibration and reconfirmed that, compared with ensemble methods, SWA is short at uncertainty calibration. Besides, we open-sourced our code to facilitate future research.

## Acknowledgment

This work was supported by Research Initiation Project (No.2021KB0PI01) and Exploratory Research Project (No.2022RC0AN02) of Zhejiang Lab.

## References

1. Bucilua, C., Caruana, R., Niculescu-Mizil, A.: Model compression. In: Proc. of the 12th ACM SIGKDD. pp. 535–541 (2006)
2. Caruana, R., Niculescu-Mizil, A., Crew, G., Ksikes, A.: Ensemble selection from libraries of models. In: ICML. p. 18 (2004)
3. Deng, J., Dong, W., Socher, R., Li, L., Li, K., Fei-Fei, L.: Imagenet: A large-scale hierarchical image database. In: CVPR. pp. 248–255. Ieee (2009)
4. Dietterich, T.G.: Ensemble methods in machine learning. In: International workshop on multiple classifier systems. pp. 1–15. Springer (2000)
5. Džeroski, S., Ženko, B.: Is combining classifiers with stacking better than selecting the best one? Machine Learning **54**(3), 255–273 (2004)
6. Fort, S., Hu, H., Lakshminarayanan, B.: Deep ensembles: A loss landscape perspective. arXiv preprint arXiv:1912.02757 (2019)
7. Gal, Y., Ghahramani, Z.: Dropout as a Bayesian approximation: Representing model uncertainty in deep learning. In: ICML. pp. 1050–1059. PMLR (2016)
8. Garipov, T., Izmailov, P., Podoprikhin, D., Vetrov, D., Wilson, A.G.: Loss surfaces, mode connectivity, and fast ensembling of dnns. In: Advances in Neural Information Processing Systems. pp. 8803–8812 (2018)
9. Guo, C., Pleiss, G., Sun, Y., Weinberger, K.Q.: On calibration of modern neural networks. In: ICML. pp. 1321–1330. PMLR (2017)
10. Guo, H., Jin, J., Liu, B.: Stochastic weight averaging revisited. arXiv preprint arXiv:2201.00519 (2022)
11. He, K., Zhang, X., Ren, S., Sun, J.: Deep residual learning for image recognition. In: CVPR. pp. 770–778 (2016)
12. He, K., Zhang, X., Ren, S., Sun, J.: Identity mappings in deep residual networks. In: ECCV. pp. 630–645. Springer (2016)

13. Hinton, G., Vinyals, O., Dean, J.: Distilling the knowledge in a neural network. arXiv preprint arXiv:1503.02531 (2015)
14. Huang, G., Li, Y., Pleiss, G., Liu, Z., Hopcroft, J.E., Weinberger, K.Q.: Snapshot ensembles: Train 1, get M for free. In: International Conference on Learning Representations (2017)
15. Huang, G., Liu, Z., Van Der Maaten, L., Weinberger, K.Q.: Densely connected convolutional networks. In: CVPR. pp. 4700–4708 (2017)
16. Izmailov, P., Podoprikhin, D., Garipov, T., Vetrov, D., Wilson, A.G.: Averaging weights leads to wider optima and better generalization. In: Proceedings of Conference on Uncertainty in Artificial Intelligence (UAI). pp. 1–10 (2018)
17. Keskar, N.S., Mudigere, D., Nocedal, J., Smelyanskiy, M., Tang, P.T.P.: On large-batch training for deep learning: Generalization gap and sharp minima. In: Inter. Conf. on Learning Representations (2017)
18. Krizhevsky, A., Hinton, G.: Learning multiple layers of features from tiny images. Technical report, University of Toronto (2009)
19. Lakshminarayanan, B., Pritzel, A., Blundell, C.: Simple and scalable predictive uncertainty estimation using deep ensembles. Advances in Neural Information Processing Systems **30** (2017)
20. Loshchilov, I., Hutter, F.: SGDR: Stochastic gradient descent with warm restarts. In: International Conference on Learning Representations (2017)
21. Maddox, W.J., Izmailov, P., Garipov, T., Vetrov, D.P., Wilson, A.G.: A simple baseline for Bayesian uncertainty in deep learning. Advances in Neural Information Processing Systems **32**, 13153–13164 (2019)
22. Russakovsky, O., Deng, J., Su, H., Krause, J., Satheesh, S., Ma, S., Huang, Z., Karpathy, A., Khosla, A., Bernstein, M., Berg, A.C., Fei-fei, L.: Imagenet large scale visual recognition challenge. International Journal of Computer Vision **115**(3), 211–252 (2015)
23. Simonyan, K., Zisserman, A.: Very deep convolutional networks for large-scale image recognition. In: ICLR (2015)
24. Smith, L.N.: Cyclical learning rates for training neural networks. In: IEEE Winter Conference on Applications of Computer Vision (WACV). pp. 464–472. IEEE (2017)
25. Yang, Y., Hodgkinson, L., Theisen, R., Zou, J., Gonzalez, J.E., Ramchandran, K., Mahoney, M.W.: Taxonomizing local versus global structure in neural network loss landscapes. Advances in Neural Information Processing Systems **34** (2021)
26. Zagoruyko, S., Komodakis, N.: Wide residual networks. In: Proc. of the British Machine Vision Conference (BMVC) (2016)
27. Zhou, Z.: Ensemble methods: foundations and algorithms. CRC press (2012)